173 4/28/87 ~~86~~ EM

⑤ J-30288

DR 0212-7

DP-1740

WELDABILITY OF TRITIUM-CHARGED 304L STAINLESS STEEL

W. R. KANNE
C. L. ANGERMAN
B. J. EBERHARD

DO NOT MICROFILM
COVER

E. I. du Pont de Nemours & Co.
Savannah River Laboratory
Aiken, SC 29808

PREPARED FOR THE U.S. DEPARTMENT OF ENERGY UNDER CONTRACT DE-AC09-76SR00001

DISCLAIMER

Printed in the United States of America

Available from

National Technical Information Service
U. S. Department of Commerce
5285 Port Royal Road
Springfield, Virginia 22161

Price: Printed Copy A03; Microfiche A01

DP-1740
Distribution Category: UC-25

Reactor Repair
Tritium Embrittlement
Helium Embrittlement
Weld Toe Cracks

DP--1740

DE87 008554

WELDABILITY OF TRITIUM-CHARGED 304L STAINLESS STEEL

W. R. KANNE
C. L. ANGERMAN
B. J. EBERHARD

DISCLAIMER

Approved by:

R. L. Cook, Superintendent
Equipment Engineering

Publication Date: February 1987

E. I. du Pont de Nemours & Co.
Savannah River Laboratory
Aiken, SC 29808

PREPARED FOR THE U.S. DEPARTMENT OF ENERGY UNDER CONTRACT DE-AC09-76SR00001

ABSTRACT

Attempts to repair the wall of C-Reactor Tank at the Savannah River Plant were halted when Gas Tungsten Arc (GTA) welds joining patches to the wall developed toe cracks in the heat affected zone (HAZ). The cause of the toe cracks was investigated by welding on 304L samples that were tritium charged and aged to produce helium.

Helium embrittlement was shown to be the likely cause of weld toe cracking in C-Reactor Tank. GTA welds made on helium impregnated 304L produced toe cracks identical to those that caused leaking patches during C-Reactor Tank repair. Heating of a sample to remove deuterium and tritium without removing helium did not reduce cracking susceptibility. Low heat input and spot GTA welds also produced cracks, indicating possible problems using these techniques for reactor repair. However, cracks were not produced by solid state resistance welds, or by a very low heat GTA pass that did not produce melting. This indicates that non-melting or low tensile stress techniques could be used for repair.

These results have impact on any fusion welding program involving metal containing helium.

CONTENTS

LIST OF TABLES

LIST OF FIGURES

INTRODUCTION

The wall of C-Reactor at the Savannah River Plant was repaired in 1968 (Reference 1). A similar repair was undertaken in 1986, but was not completed at that time due to toe cracks in the repair weld HAZ. Cracks were on the tank wall side of welds joining 304L stainless steel patches to the 304 stainless steel wall. The toe cracks in the tank wall allowed gas to leak from under the patches during pressure testing. The cracks were readily detected by a dye penetrant test. Parallel-bead test welds made on the tank wall and on a patch installed in 1968 produced similar cracks. A program was initiated by the Savannah River Laboratory and by Westinghouse Electric Corp. to determine the cause of the HAZ cracks.

Among the possible causes of the cracking are helium embrittlement and hydrogen embrittlement. Hydrogen was shown to not be a cause of the observed cracking (Reference 2). Other possible causes such as intergranular attack from pickling during tank fabrication or radiation induced segregation were shown to be unlikely.

Helium is present in the reactor tank wall at concentrations of approximately 3 appm, primarily from irradiation of boron. Helium is known to reduce the ductility of 304 stainless steel at concentrations down to 0.1 appm (References 2 and 3). However, a high rate of successful welds joining uncharged endcaps to tubing with helium concentrations of 3 to 20 appm was experienced by Hall (Reference 4).

To demonstrate the role of helium in weld toe cracking, test welds were made on samples whose walls contained dissolved tritium, deuterium, and helium (from tritium decay) at high surface concentrations.

Blank Page

DISCUSSION

Description of Tests

Samples used for the welding tests had a radius of curvature of 1.375" and were 0.375" thick (C-Tank vertical wall is 0.5 inch thick). The test beads were made on the tritium exposed surface parallel to the cylinder axis and across a pre-existing GTA weld (made before tritium exposure). Aging of the samples during storage produced sharper gradients in helium and hydrogen isotopes than in the reactor wall, but the average concentrations were similar. Two of the samples, A-1 and A-2, came from the same coupon, but A-2 was heated for 24 hours at 500°C to off-gas 90% of the hydrogen without affecting the helium content. The third sample, B-1, was from a second coupon with about 80% of the helium content of the first.

Parallel-bead test welds were made on the samples using the equipment shown in Figure 1. The welding power supply was a Hobart 300 amp DC Cyber-tig equipped with an 800-Series Programmer, which permitted pulsing of the weld current, up and down slope, and other features required for automatic welding. The first two welds on each piece were made at parameters chosen to duplicate those made in C-Tank, as shown in the first three lines of Table 1. Control tests on unexposed 304L pipe and on the unexposed outside of one of the samples did not result in cracking, as shown by dye penetrant tests. Each of the test beads was examined for cracks by direct visual inspection, dye penetrant tests with Magnaflux spray, and by metallographic sections.

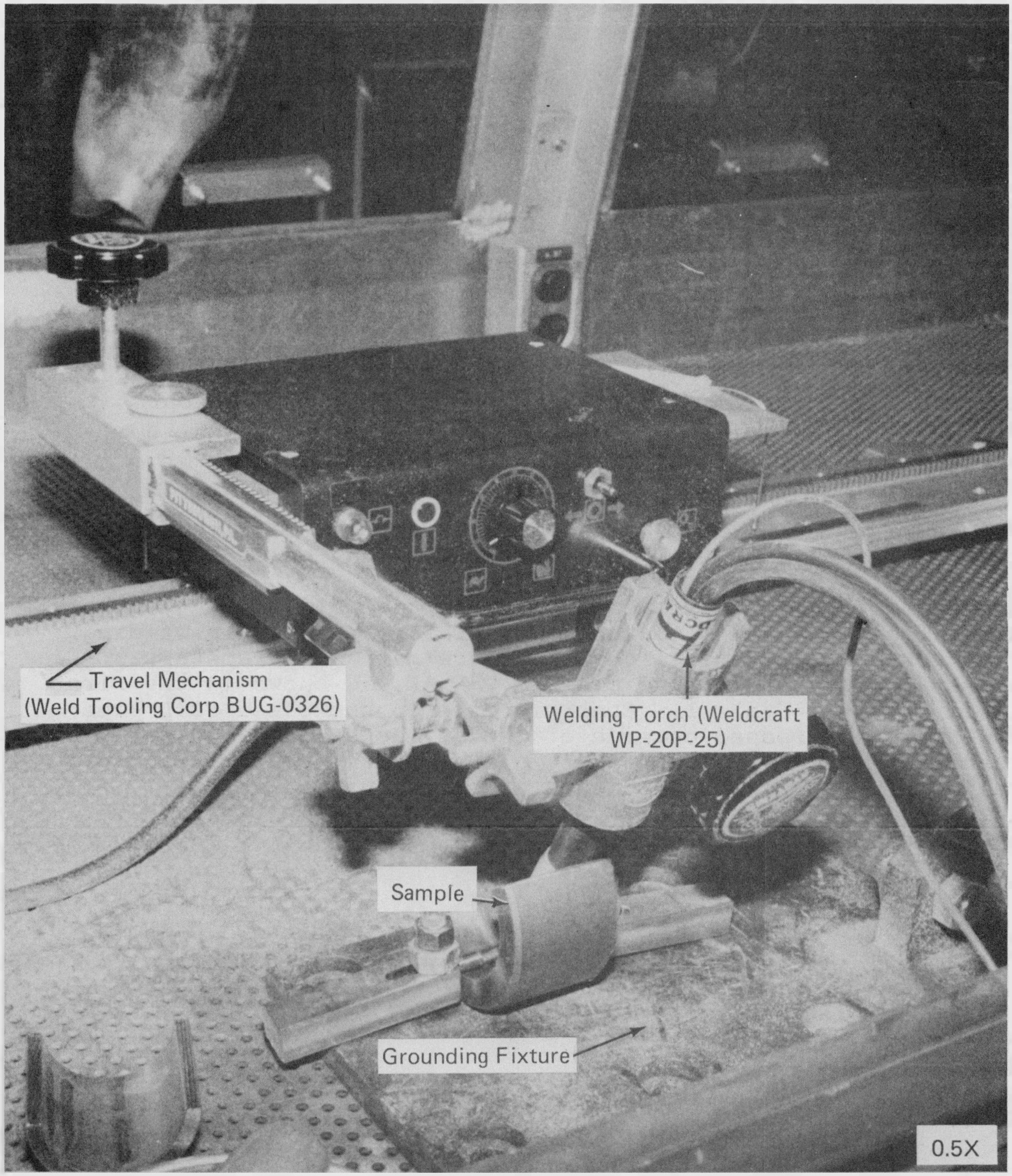

FIGURE 1. Welding Station in Glove Box

TABLE 1

WELD DATA FOR TRITIUM CHARGED MATERIAL

PLATE: WELD NO.	CURRENT, A	VOLTAGE, V	SPEED, 1PM	HEAT INPUT KJ/IN	MAXIMUM OBSERVED CRACK DEPTH, IN
A-1:A,B*	205/105	10/7.6	2	40.9	0.035
A-2:A,B	205/105	10/7.6	2	40.9	0.032
B-1:A,B	205/105	10/7.6	2	40.9	0.022
B-1:C	60/35	9.8/9.0	4	6.7	0.015
A-2:C	60/35	9.8/9.0	4	6.7	0.020
B-1:D	92/50	9.2/8.4	4	9.4	0.020
B-1:3	45/23.4	11/10	4	5.4	
A-2:D	22.4**	12.3	3	5.5	
A-2:E	205	SPOT	0		
A-2:F	100	SPOT	0		

* APPLIED DOUBLE PASSES ON EACH WELD BEAD
** NO PULSING

Simulated C-Tank Welds

Welds made with heat inputs similar to those used in repair of C-Tank produced toe cracks similar to those in C-Tank, as shown by dye penetrant tests, Figure 2. Double parallel beads (parallel beads with a second pass on top of each) were made on piece A-1, Figure 3. The cracks, which were not visible to the unaided eye, were largest toward the end of the weld, but did not necessarily occur on both sides of a bead. Cracks were present in the pre-existing GTA weld (charged with tritium and helium) where the double parallel bead welds crossed it, but these cracks were not continuous. Crack depths observed metallographically ranged up to 0.035 inch, Figure 4. Their path was intergranular and generally perpendicular to the surface (e.g., not along the fusion line of the weld). These cracks did not appear to be advancing along grain boundaries decorated with visible gas bubbles (at 1000X magnifications). Considerable porosity was present within the weld.

Low Heat Input Welds

Welds made on piece B-1 showed that the double bead is not necessary for cracking, that low heat welds crack like high heat welds, and that cracking occurs beyond the end of melting. On this piece, beads A and B, Figure 5, were made at the same parameters as those for piece A-1 but were not overlayed with a second bead. Beads C through E were made with lower heat inputs produced by lower currents and faster travel speeds, Table 1. The lowest heat input (Bead E) did not result in continuous melting. The dye penetrant test showed cracks around all five welds, Figure 6.

Cracks produced by these welds were generally smaller than those in piece A-1, both in depth (up to 0.020 inch, Table 1) and in width of opening at the surface. Cracks typical of those around beads A and B are shown in Figure 7. In the low heat input welds, cracks were seen in regions just barely melted and beyond the ends of the welds, Figure 8.

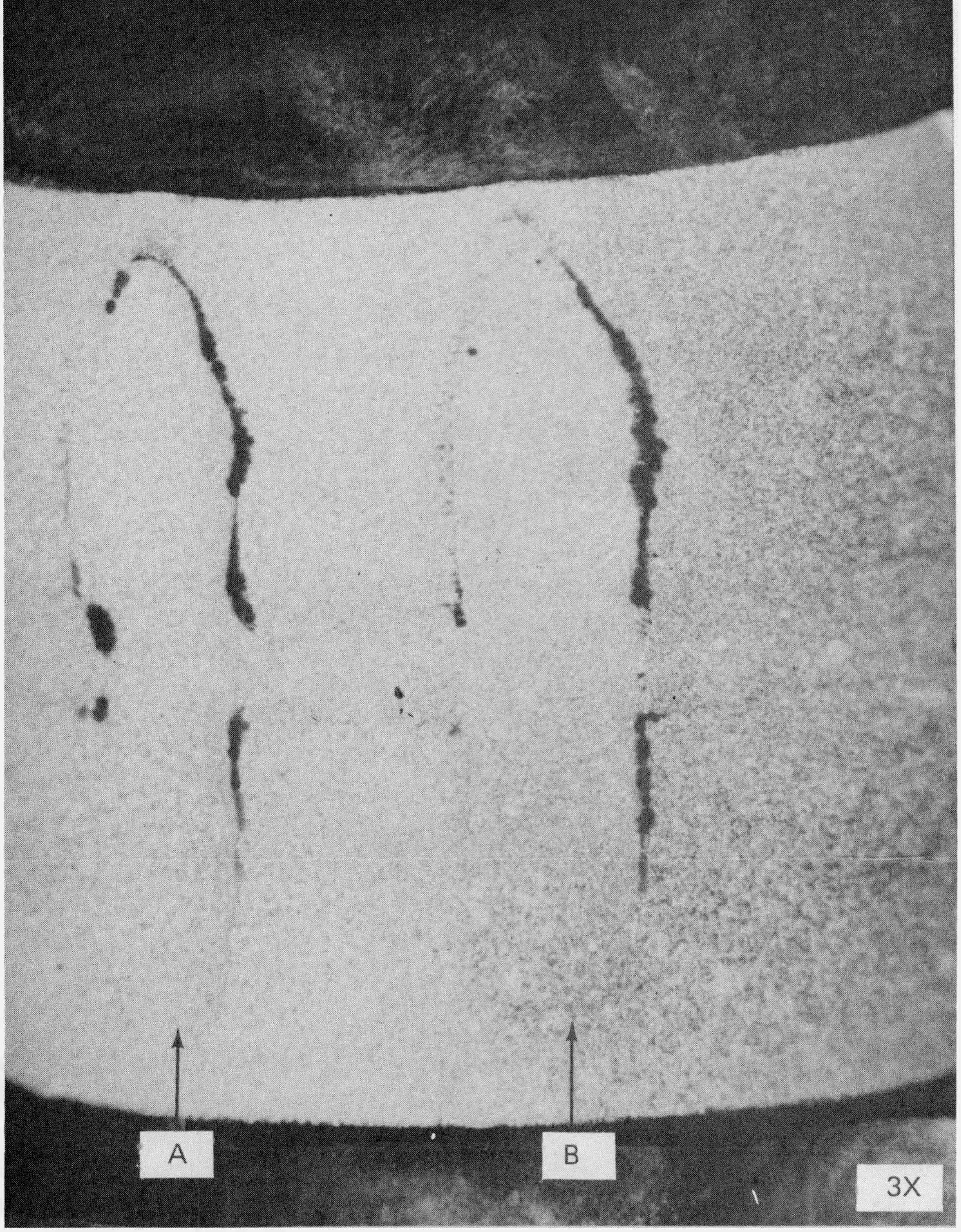

FIGURE 2. Dye Penetrant Test of Piece A-1

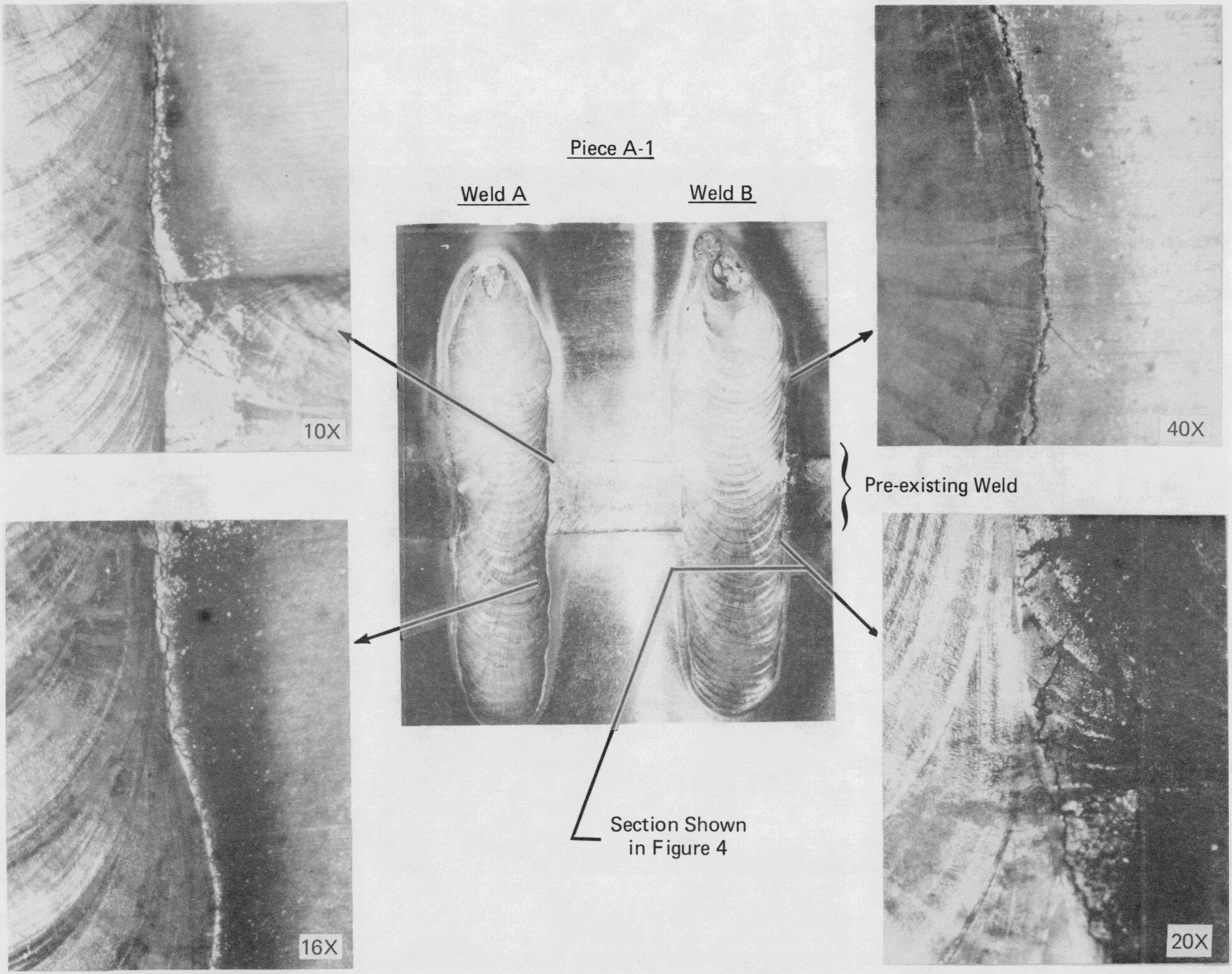

FIGURE 3. Toe Cracks Produced at C-Tank Welding Conditions, Piece A-1

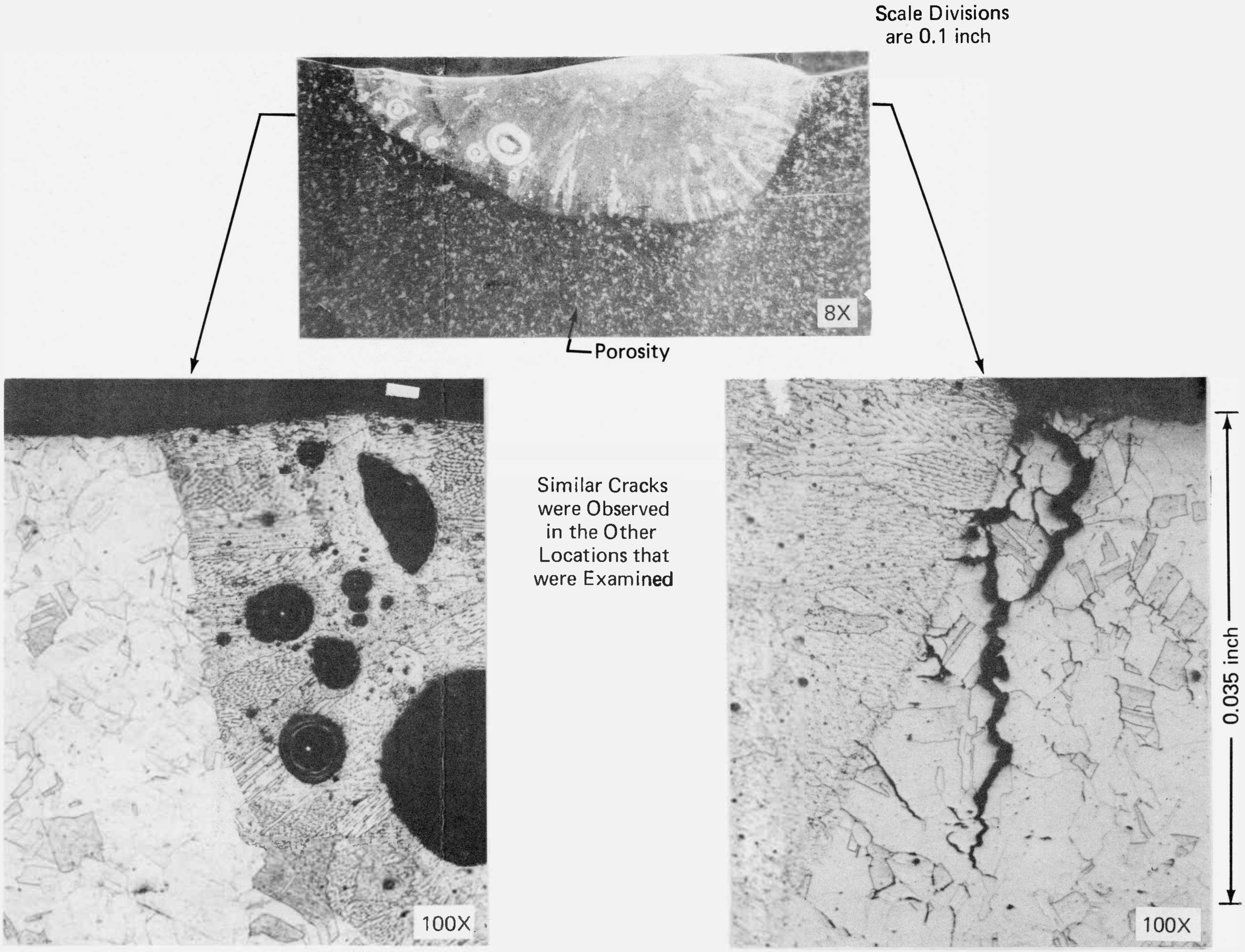

FIGURE 4. Typical Toe Crack and Porosity at C-Tank Conditions, Piece A-1

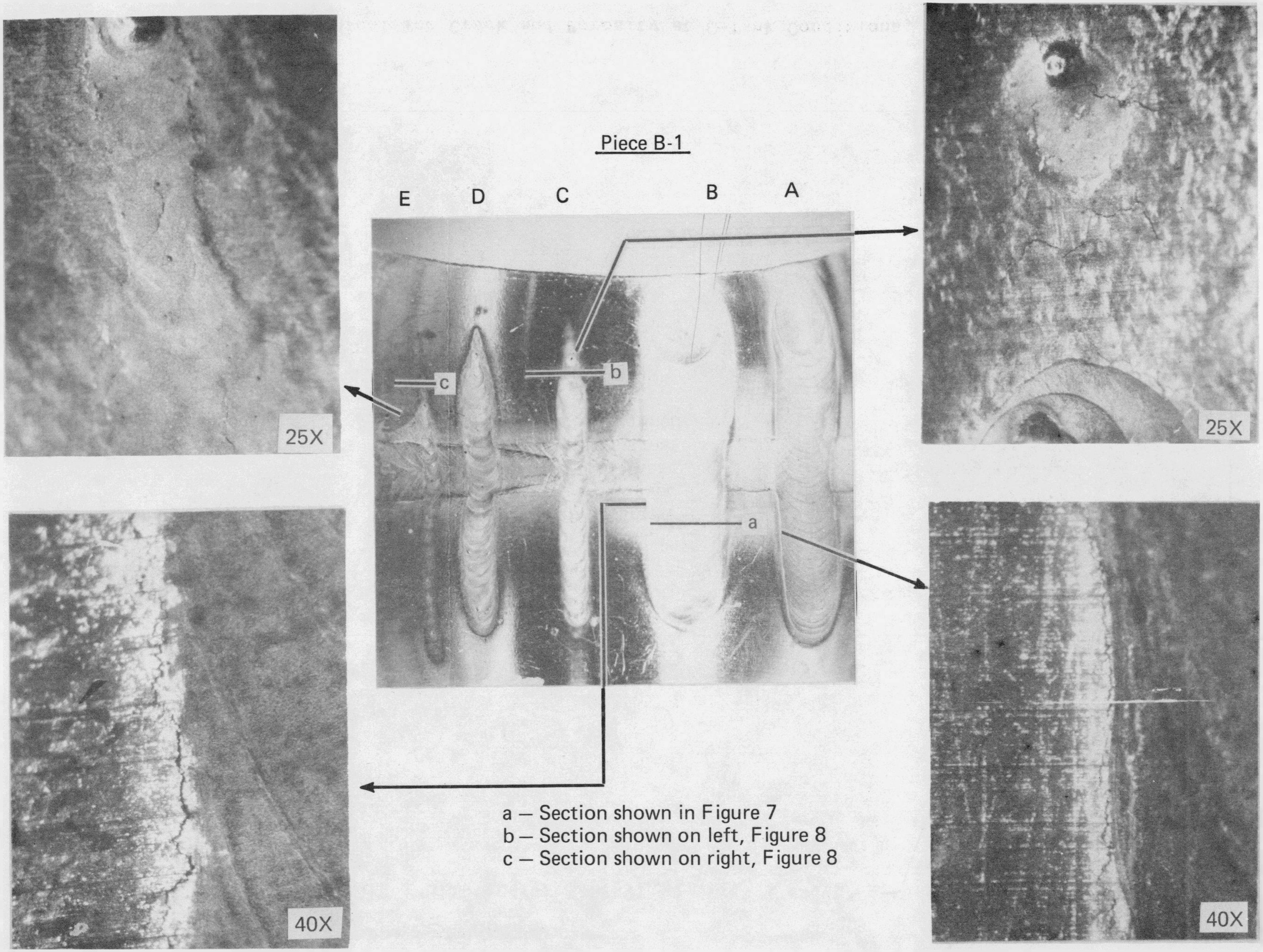

FIGURE 5. Cracking Produced by Low Heat Welds, Piece B-1

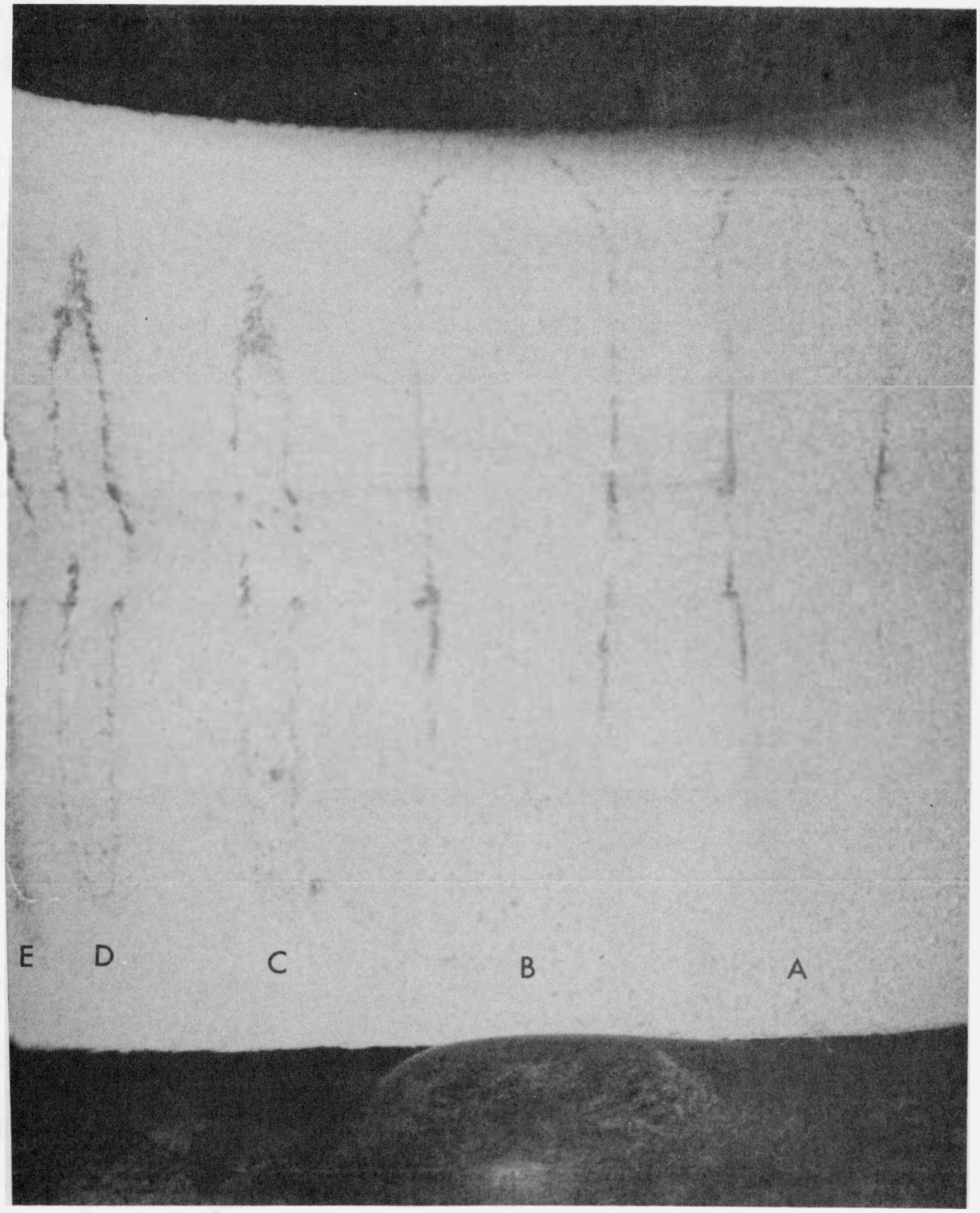

FIGURE 6. Dye Penetrant Test of Piece B-1

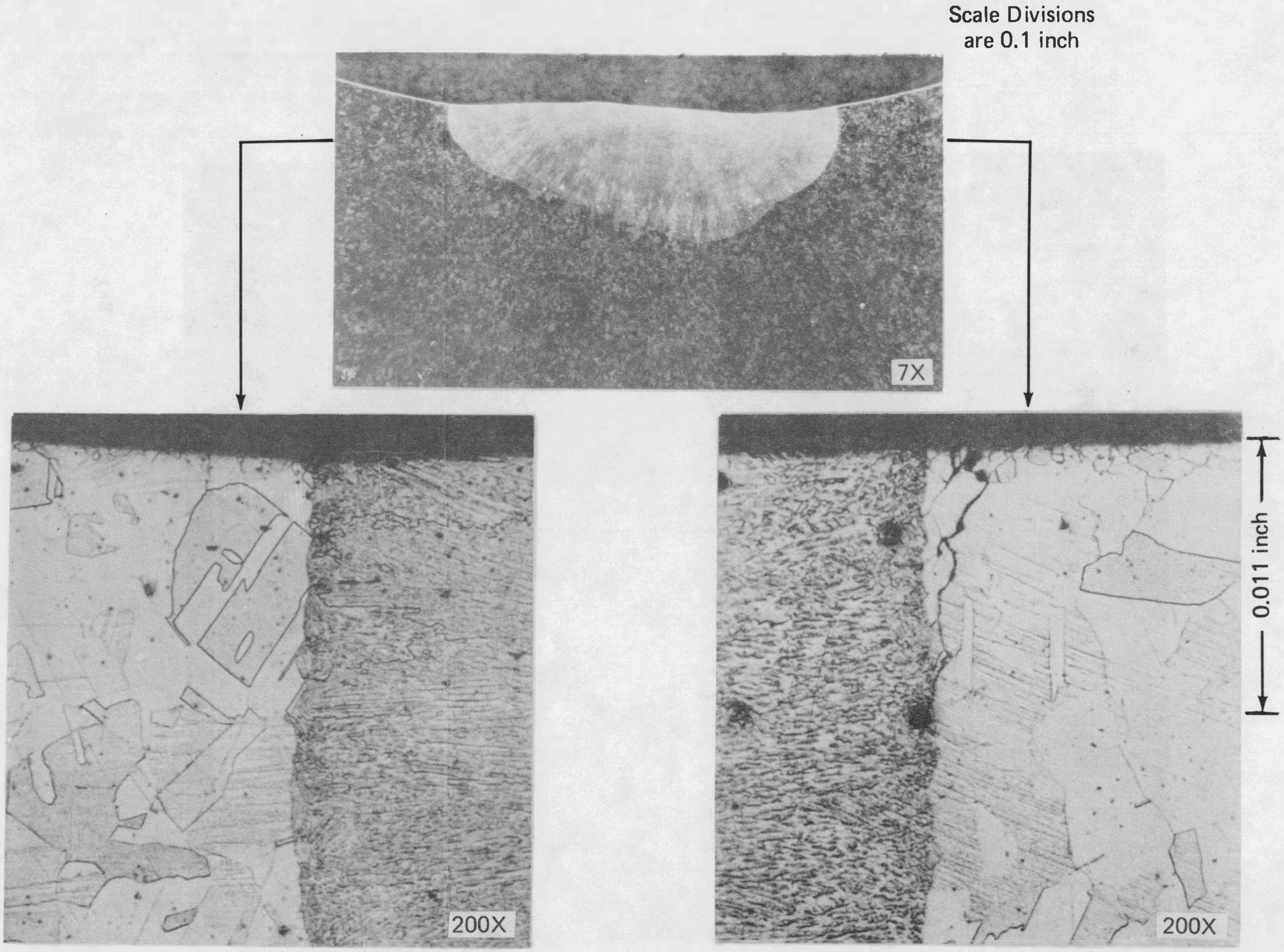

FIGURE 7. Toe Crack Typical of Welds A and B, Piece B-1

Weld C

Weld E

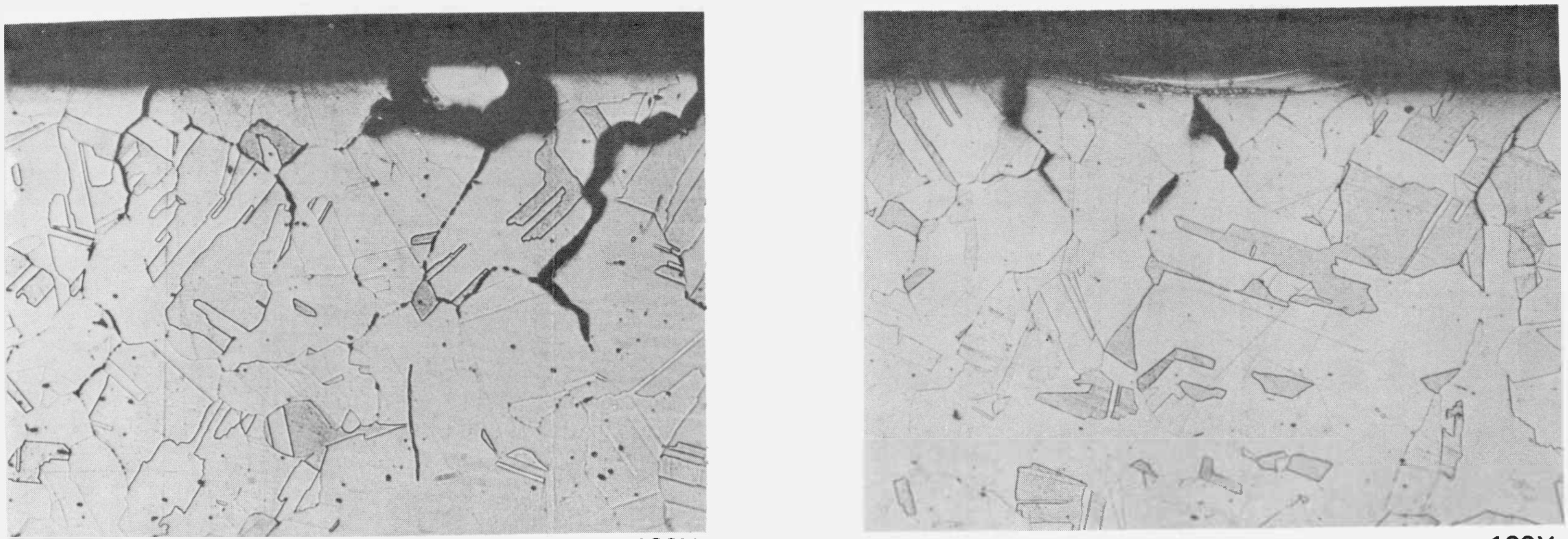

100X

100X

Surface Cracks in Unmelted Region

Surface Cracks Associated with Only Surface Melting (Center of Photo)

FIGURE 8. Cracking at Low Heat Input Welds, Piece B-1

Cracking Due to Helium Alone

Both high and low heat input welds caused cracking in piece A-2, which had been off-gassed to remove 90% of the hydrogen, Figures 9 and 10. This result suggests that helium embrittlement is the principal cause of the cracking. As with the samples containing both helium and hydrogen (A-1 and B-1), cracks were intergranular and were deeper around high heat welds than those around the low heat weld (0.032 inch compared to 0.020 inch), Figure 11. The degree of porosity within the weld bead was not noticeably different. Two spot welds made at different heat inputs, Table 1, also resulted in cracking.

Non-Melting Weld Techniques

Two techniques did not result in cracking. One technique was resistance welding. Resistance welds (Figure 12) were made by attaching tubes to the surface of piece A-1 using a technique developed previously (Reference 5). Welding conditions were 1000 lbs. force and 8000 amps current for 0.5 sec. A solid state weld was formed joining the tube to the sample surface, Figure 13. A flash of molten metal around the weld perimeter did not have any porosity. Neither dye penetrant nor metallographic examinations showed any cracking associated with the weld.

The second non-melting technique used the welding torch to just heat a sample to simulate heating during brazing. The sample (A-2, pass D) was oxidized along the path of the torch, but no weld bead formed. The path was parallel to and within 0.25 inch of a fusion weld bead that had cracked. No cracking was found along the path heated by the welding torch by either dye penetrant or metallographic examinations.

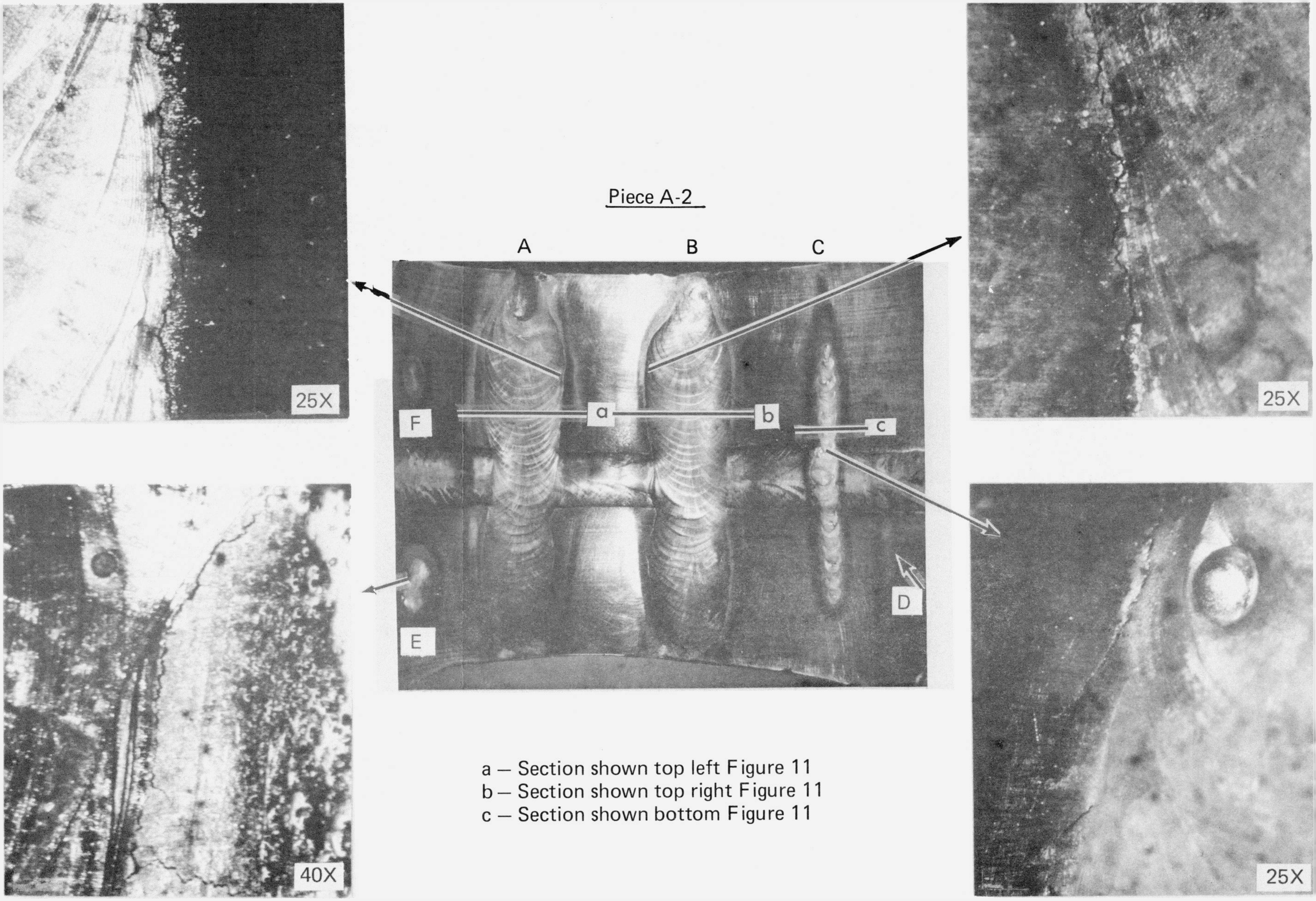

FIGURE 9. Toe Cracks Caused by Helium Alone, Piece A-2

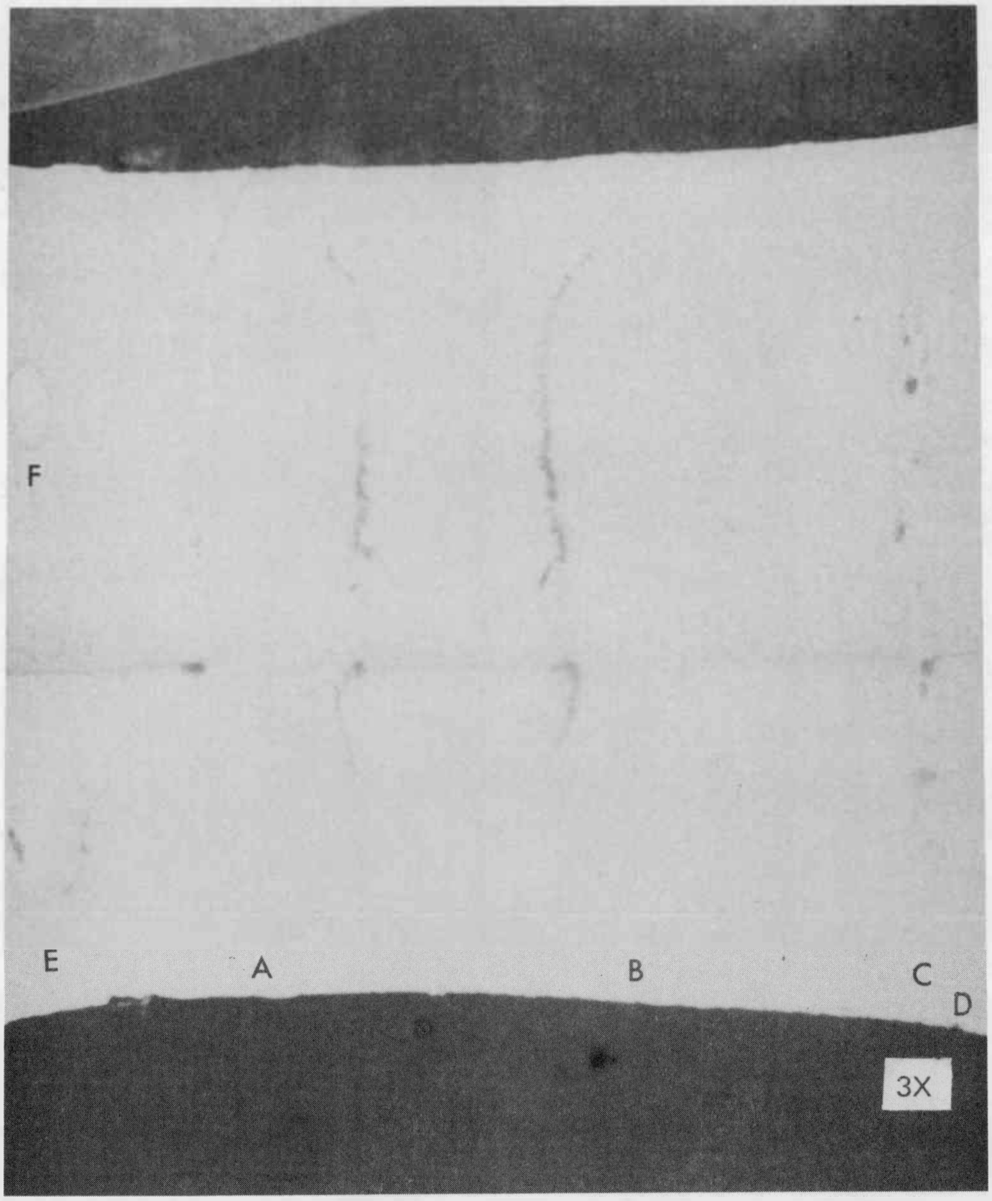

FIGURE 10. Dye Penetrant Test of Piece A-2. Weld Pass D did not Show Dye and is not Visible in this Photo

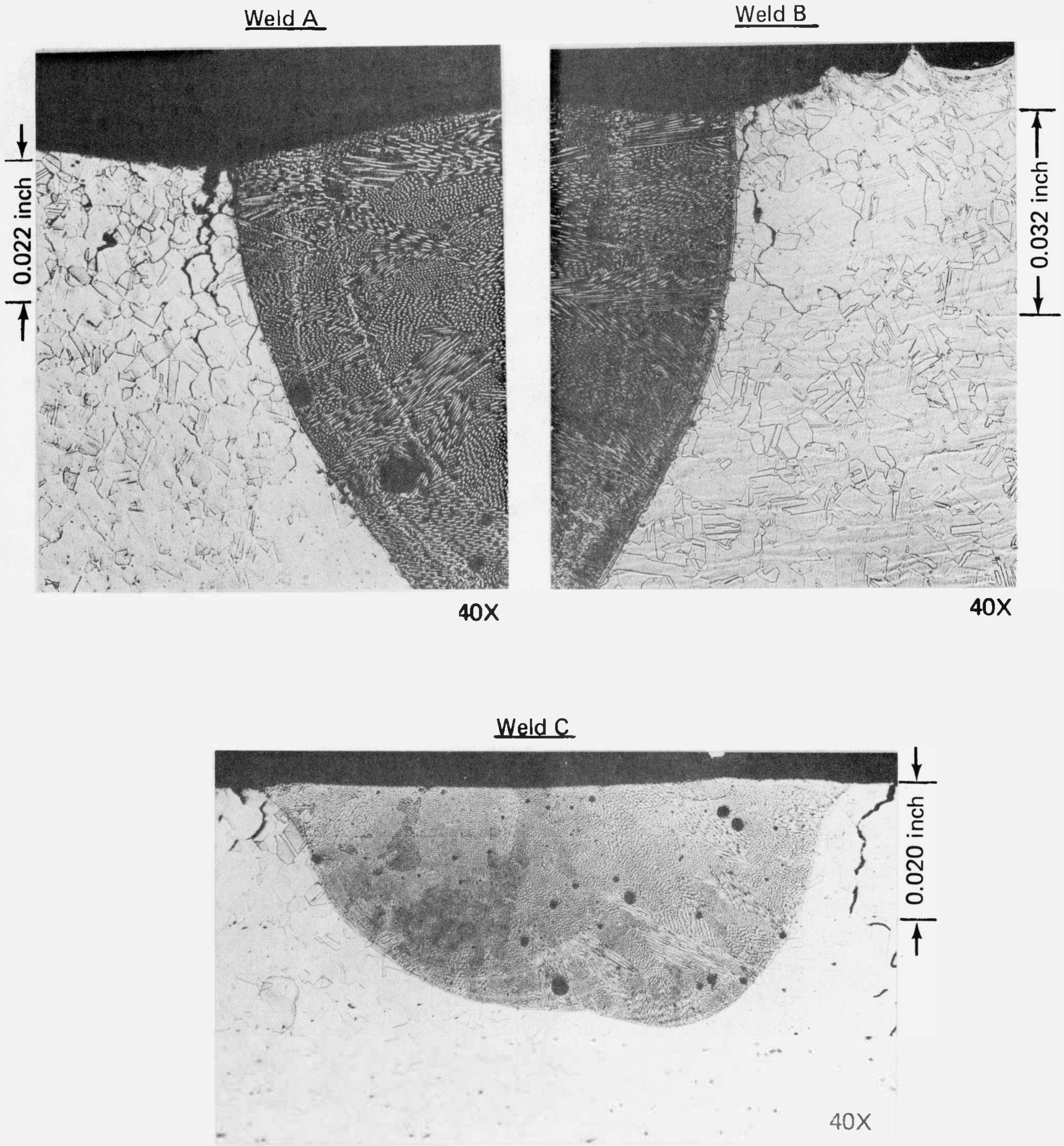

FIGURE 11. Intergranular Cracks from Helium, Piece A-2

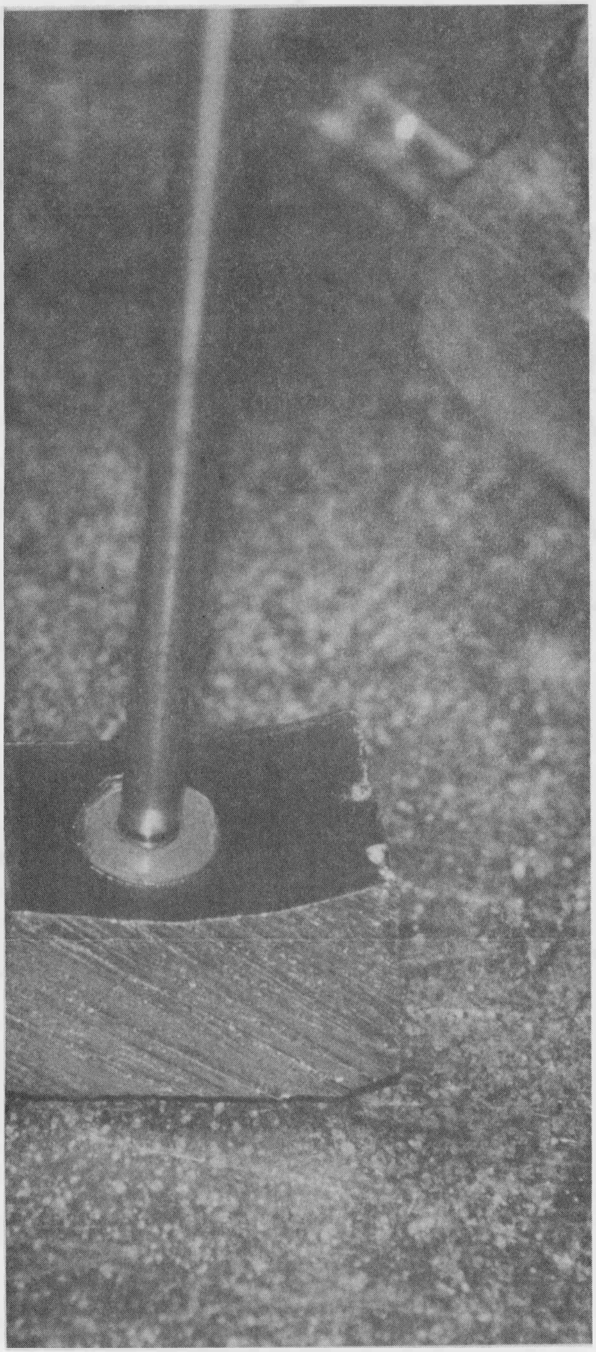

FIGURE 12. Resistance Welds Joining Tubes to Sample Surface

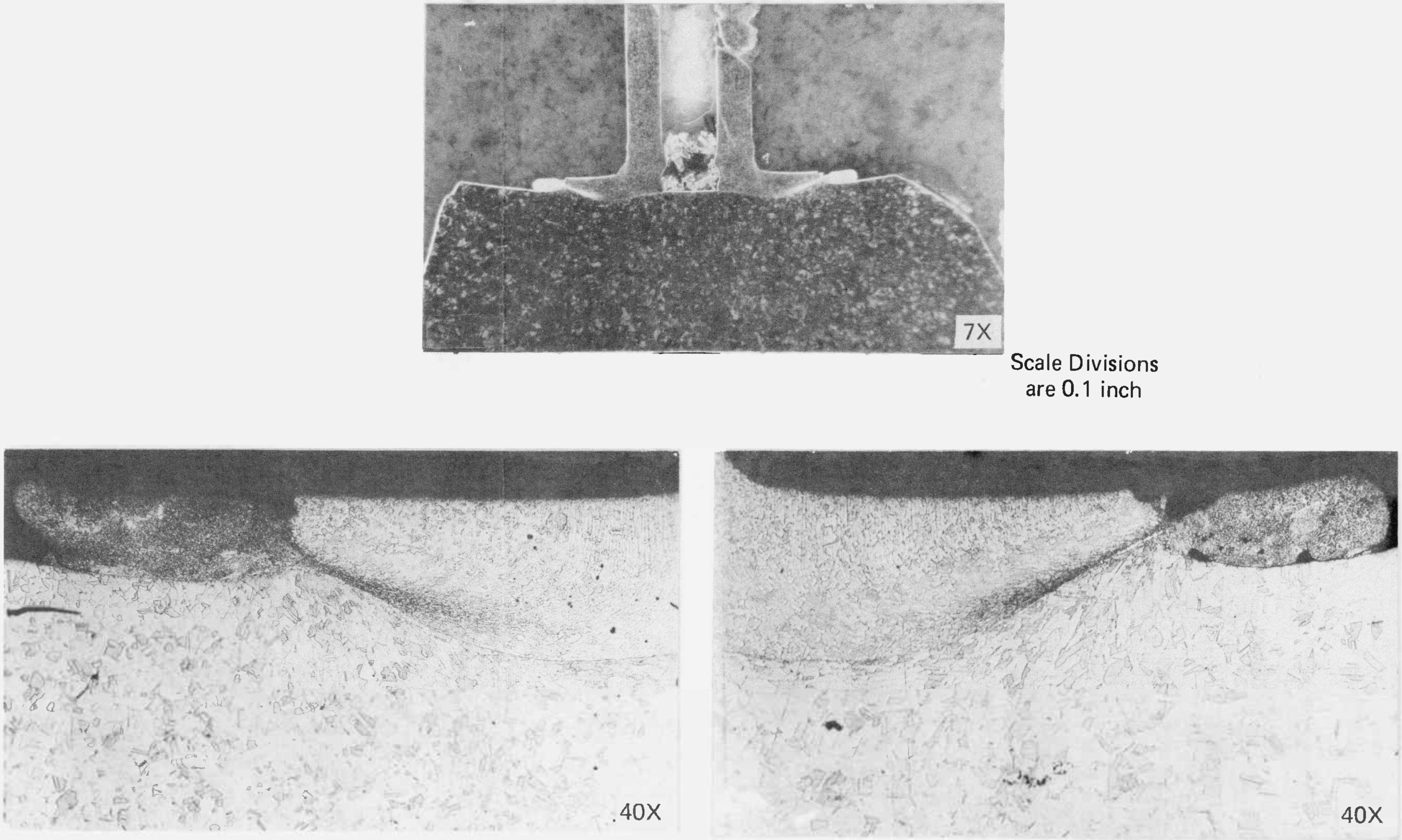

FIGURE 13. Crack-Free Resistance Weld. Solid State Weld (Center) with Flash of Molten Metal at Outer Edge.

CONCLUSIONS

The following conclusions can be drawn from this study:

- Toe cracks like those in C-Tank resulted from the presence of helium with little, if any, assistance from hydrogen.
- Cracking was not eliminated by single pass welds, low heat input welds, or spot welds.
- No cracking was seen when base metal temperatures below melting were maintained, such as resistance welding or simulated brazing.

REFERENCES

1. J. P. Maloney, et al., Repair of a Nuclear Reactor Vessel, DP-1199, E. I. du Pont de Nemours & Co., Savannah River Laboratory, Aiken, SC, (June 1969).

2. A. K. Birchenall, et al., Savannah River Laboratory, Private Communication.

3. D. Kramer, et al., "Helium Embrittlement in Type 304 Stainless Steel," Journal of Nuclear Material, 25, pp 121-131, 1968.

4. M. R. Louthan, Jr., et al., "Tritium Effects in Austenitic Steels," Proceedings of the Conference on Radiation Effects and Tritium Technology for Fusion Reactors, IV, CONF-750989, pp 98-116, (March 1976).

5. M. M. Hall, Jr., et al., "Fusion Welding of Irradiated AISI 304L Stainless Steel Tubing," Weldments: Physical Metallurgy and Failure Phenomena, Proceedings of the Fifth Bolton Landing Conference, pp 365-378 (August 1978).

6. W. R. Kanne, Jr., "Solid State Resistance Welding of Cylinders and Spheres," Welding Journal, pp 33-38, (May 1986).

DISTRIBUTION

1-8 DOE

9-12 Wilm.

13-72 SRL File
73 W. S. Shingler, Mosd. 5-35, Westinghouse Electric Corp., 2400 Mosside Blvd. Monroeville, PA 15146
74 P. S. Marin, Mosd. 5-35
75 E. Haberman, Mosd. 3-24

76 R. J. Jacko, R&D 401 2A58, Westinghouse Electric Corp., 1310 Beaulah Rd, Pitts, PA 15235
77 R. P. Shogan, R&D 302 203
78 G. G. Lessmann, R&D 501 1Y62
79 P. E. Denney, R&D 501
80 D. A. DelSignore, R&D 701-208

81 C. Bagnall, Large - Westinghouse Electric Corp., Bldg. 5, Box 10864, Pittsburgh, PA 15236
82 R. Bajaj, Large - Bldg. 5

83 E. A. Franco-Ferreira, E. F. Enterprises, 1047 Hygeia Avenu, Leucadia, CA 92024

84 D. Warren, 436 Garland Rd., Wilmington, DE 19803

85 J. K. Roberts, Atomic International, Rocky Flats Plant

86 C. B. Banks, Jr., Los Alamos National Laboratory
87 K. F. Wylie
88 L. C. Michels
89 R. A. Patterson

90 R. W. Rhode, Sandia National Laboratory Livermore
91 J. A. Brooks
92 M. W. Perra
93 E. T. Cull
94 H. Hanser
95 L. N. Tallerico
96 J. R. Spingarn

97 K. Farrell, Oak Ridge National Laboratory
98 G. M. Slaughter
99 G. M. Goodwin

100 W. H. Jones, Mound Facility

101-274 DOE-OSTI, Standard Distribution under Category UC-25